

## Design and Construction of the Tuning Fork Piezoelectric Motor

PACS REFERENCE: 85.50.-n  
Friend, James R.<sup>1</sup>; Satonobu, Jun<sup>2</sup>; Nakamura, Kentaro<sup>1</sup>; Ueha, Sadayuki<sup>1</sup>; Stutts, Daniel S.<sup>3</sup>

<sup>1</sup>Tokyo Institute of Technology  
Precision and Intelligence Laboratory  
4259 Nagatsuta-cho, Midori-ku  
Yokohama, JAPAN 226-8503  
Tel: +81 (45) 924-5052  
e-mail: jamesfriend@ieee.org

<sup>2</sup>Hiroshima University  
Department of Mechanical Engineering  
Hiroshima, JAPAN 739-8527

<sup>3</sup>University of Missouri-Rolla  
Department of Mechanical and Aerospace Engineering and Engineering Mechanics  
Rolla, Missouri 65401 USA

### ABSTRACT

This paper describes the design of a piezoelectric tuning-fork dual-mode motor. The motor uses a single multilayer piezoelectric element in combination with tuning fork and shearing motion to form an actuator using a single drive signal. Finite-element analysis was used in the design of the motor, and the process is described along with the selection of the device's materials and its performance. Prototypes of the actuator achieved a maximum linear no-load speed of 13 *cm/s*, a maximum linear force of 5.98 *N*, and a maximum efficiency of 25%.

### INTRODUCTION

Piezoelectric motor systems exploit the transduction phenomenon from electrical energy input to mechanical energy output within piezoelectric materials. The solid-state construction possible with such devices coupled with their peculiar advantages over standard electromagnetic motors is constrained by their sensitivity to heat, relatively low efficiency, and short operating life [1]. However, inroads are being made on these problems, and commercially useful actuators are becoming more common. This paper presents a design that marks a small step in this process; it details the design, construction, and testing of a small single-piezoelectric element linear actuator for low-voltage applications, using, to the knowledge of the authors, previously unpublished construction techniques.

Alps Corporation developed a small linear motor system [2,3] that moves a slider with decent traction and speed using either one or two multilayer piezoelectric actuators (MLPA). However, the Alps designs allow one end of the piezoelectric actuation material to be left free, allowing a significant amount of the vibration energy generated by the material to be lost. Inherent in the proposed design is the use of a single MLPA enclosed in a structure, which, when operated at the design frequencies of the actuator, uses comparatively low voltages, roughly 5  $V_{RMS}$  versus 100  $V_{RMS}$  for a 40 *mm* Shinsei motor. The mounting technique places the piezoelectric material in compressive prestress and makes use of both ends of the MLPA. This serves as an advantage in high-altitude, spacecraft, or Martian atmospheres where ionization of the gas surrounding the actuator could permit arcing even at modest voltages [4], and that advantage is one of the reasons for pursuing this study.

## DESIGN

The initial concept of the tuning fork device was developed to retain the traditional arrangement of a piezoelectric motor: piezoelectric material exciting an ultrasonic vibration in a metal *stator* to move relative to a surface in contact, the *slider*, with the stator. Figure 1 illustrates the initial concept of the tuning fork actuator.

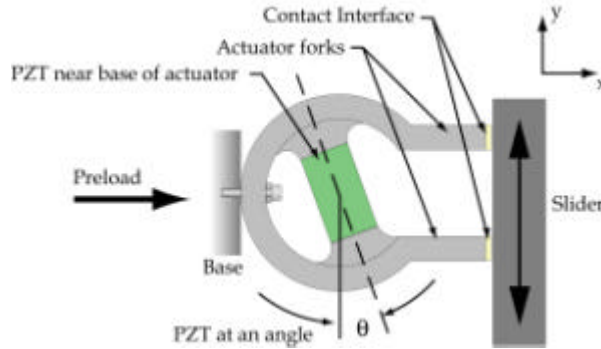


Figure 1: Initial concept of the tuning fork device

If the MLPA is forced to vibrate in its fundamental breathing mode along its long axis, indicated by the dashed line in Figure 1, both ends of the MLPA serve to excite vibration in the surrounding stator structure. By placing the piezoelectric material at an angle, simple tuning fork motions married with lifting motions of the forks can generate elliptical motion along the contact interface that can be used to move the slider in both directions. It is important to note some of the mode shapes of the structure do not possess tuning fork or lifting motion, instead having significant out-of-plane motion or motion contained mostly within the hoop section of the stator. Avoiding those modes is an important part of the design as well.

The motor can be described in an abstract sense with a set of parameters that define its geometry. Using a linearly independent set of parameters—the *basis*—the quality of the motor design can be associated with an objective function dependent on this basis, permitting the selection of a superior design based on analysis results. The objectives of such an analysis would be to maximize the magnitude of output motion and align the frequencies of the desired resonant modes. One possible basis for the geometry of the tuning fork stator is shown in Figure 2.

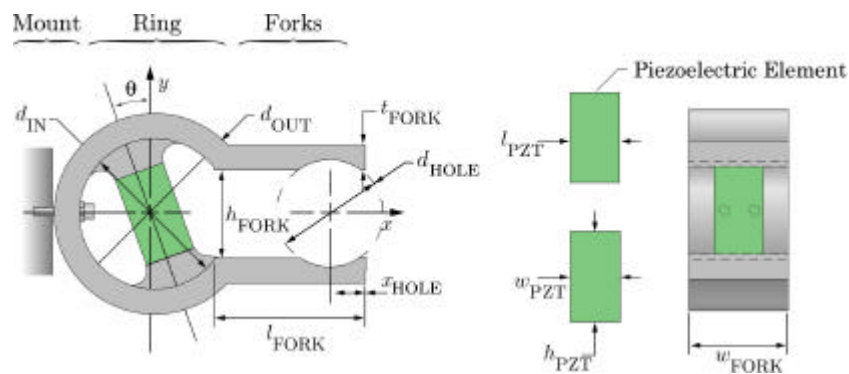


Figure 2: Definition of parameters used to describe the geometry of the actuator

This set of twelve parameters, with the overall scale of the device serving as the thirteenth, is convenient for defining the stator's geometry. By doing so, the design could be altered by changing the magnitude of the variables, within limits imposed to ensure selection of a geometry that could be constructed. The parametric design study was carried out using modal and harmonic finite element analysis. The design objectives included the following: increasing the frequencies of useful modes beyond the audible range, discouraging out-of-plane motion and

vibration near the mounting, and maximizing the desirable output motion along the contact interface.

Early in the design analysis, the resonance frequencies were found to be in the audible range for practical choices of transducer materials. To remedy this problem, a thin rib was placed across the forks near the piezoelectric element. The fundamental tuning fork resonance frequency increased from near  $9.8\text{ kHz}$  to beyond  $25\text{ kHz}$  with the introduction of a  $2\text{ mm}$  thick web. This part also permits adjustment of the resonance frequencies after assembly by polishing or drilling to change its stiffness.

Since the piezoelectric element is turned at an angle  $q$  with respect to the actuator's main axis, the actuator is asymmetric. This asymmetry is beneficial for lifting the forks of the actuator, but the motion of one fork relative to the other becomes asymmetric as well. Further, the asymmetry causes a splitting of the degenerate "tuning fork" mode into two separate modes, each having combined tuning fork/lifting motions, with motion in only a single fork. This effect is seen in not only the fundamental tuning fork mode but also in the higher order modes. To address this problem, material was removed from the circular section of the actuator on the side where the PZT is closer to the end of the fork; this acts to lower its stiffness to match the other side of the actuator where the end of the PZT is nearer the base. On that side of the actuator, material was removed from the fork to lower its mass to increase its apparent stiffness. These two changes, combined together, compensated for the asymmetry of the design. Figure 3 illustrates the effect with results from finite element analysis.

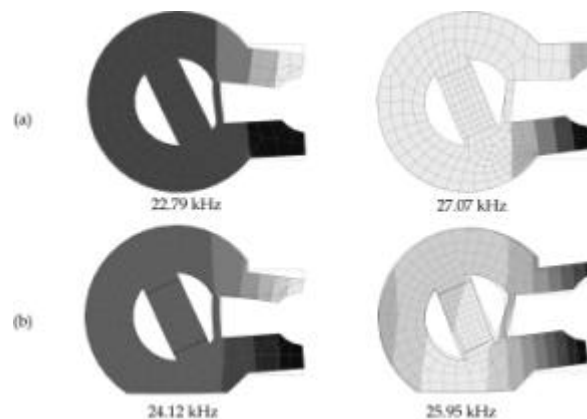


Figure 3: Compensating for the asymmetry in the stator; finite element analysis results of the first two tuning/lifting fork modes (a) with no compensation, (b) with grinding of the top fork ( $1.5\text{ mm}$ ) and bottom of the ring section ( $2\text{ mm}$ ).

The ratio of maximum displacement of the top fork tip to the bottom fork tip in the  $y$ -direction was originally 2.02 for  $22.7\text{ kHz}$  and 5.8 at  $27.1\text{ kHz}$ , but became 1.58 at  $24.1\text{ kHz}$  and 1 at  $25.9\text{ kHz}$ , respectively, after grinding away  $1.5\text{ mm}$  of the top fork and  $2\text{ mm}$  along the bottom of the ring section of the actuator. Note further that the resonance frequencies of the two modes are much closer together.

## ACTUATOR CONSTRUCTION

The stator was machined using CNC milling of C1020 low-corrosion steel plate. The fork tips and MLPA mounts were polished to a mirror or  $5\text{ }\mu\text{m}$  finish in preparation for mounting the friction material and the MLPA. The MLPA was placed within the stator and checked for a snug fit, taken out and replaced with Loctite H-20EP epoxy along the interfaces between the MLPA and stator, and mechanically secured in place by swaging the stator at two or more places near the mounting interfaces. Though it is probably possible to eliminate the use of epoxy to bond the MLPA to the stator, it was not tried for these prototypes. Two materials were used for contact on the stator, alumina, and asbestos brake liner material. For the slider, alumina was used throughout.

## RESULTS

The impedance characteristics of the actuator were measured using a standard HP4194A analyzer at  $0.5V_{RMS}$ . As might be expected, placing the stator into contact with a slider caused significant change in the impedance spectrum, as illustrated in Figure 5.

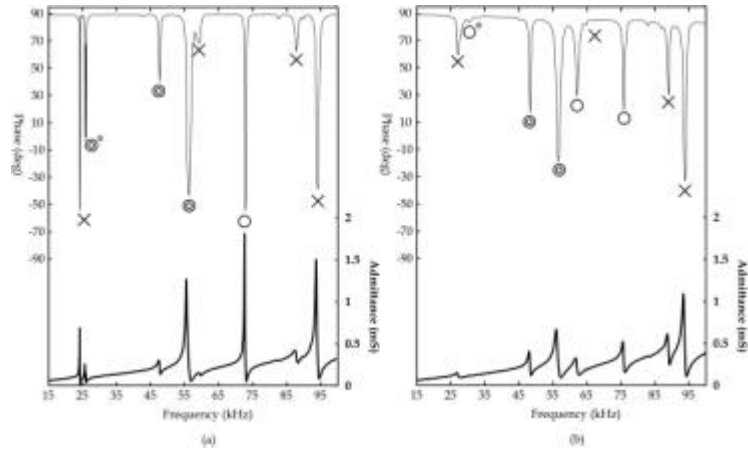


Figure 5: Impedance amplitude and phase characteristics of the stator with respect to excitation frequency (a) without slider and (b) with a slider at 1.98 N preload

The contact interface was alumina/alumina, though other contact interfaces produced similar results. The response of the stator spread out across more modes when placed against the slider, with some formerly insignificant vibration modes at 47, 62, and 87 kHz becoming more prominent. In particular, the mode at about 47 kHz amplified enough to become useful as will be shown below. Unfortunately, the reverse is also true; several modes that appeared useful without the slider almost disappeared when the slider was introduced, especially the fundamental mode at about 27 kHz, indicated with an asterisk in Figure 5. The single and double circular marks indicate useful and ideal modes, respectively, while the crosses indicate modes that appear to be useless for actuation, according to the finite element analysis results described in the previous section. Certainly the introduction of the slider alters these mode shapes, just as it has altered the impedance spectrum, but the effect was not included in the finite element analysis due to the extraordinary expense of contact analysis.

Using a custom-built test fixture, measurements of the slider's velocity with respect to time, preload, voltage applied to the MLPA, stator version, and mass on the monofilament line were made. From these measurements, the axial force the stator could deliver to the slider based on these variables was determined. Figure 6 illustrates the velocity of the slider from the first detection of motion by the encoder until the slider reached its end stop for several different string masses.

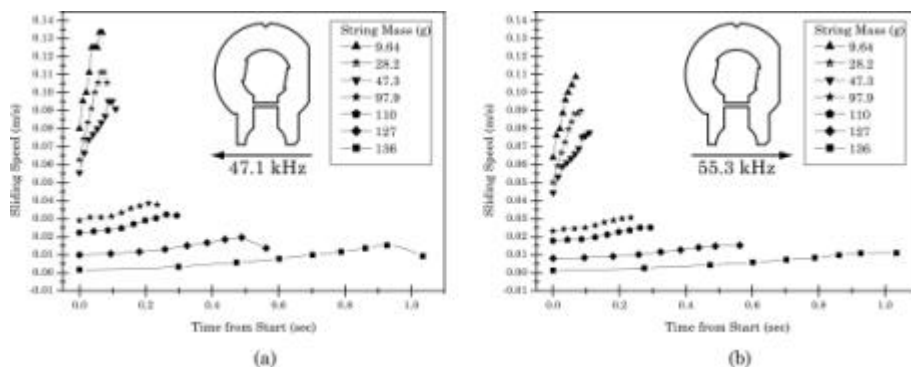


Figure 6: Velocity of slider versus time from start of sliding measurement for different masses pulling on the slider under gravity, with brake liner/alumina contact counterfaces, at (a) 47.1 kHz and (b) 55.3 kHz

The brake liner/alumina contact interface was used, with a preload of 6.7 N, and a 3.5  $V_{RMS}$  sinusoidal signal applied to the MLPA of at either 47.1 kHz or 55.3 kHz. The results indicate an inverse relationship between the generally linear acceleration of the slider and the mass on the line, as might be expected. Further, the acceleration and maximum velocities of the actuator at 55.3 kHz are approximately 80% of the response at 47.1 kHz. Figure 7 shows the results of using different preload forces on the sliding force and efficiency versus the peak velocity of the slider. Here, the maximum velocity reached by the slider is different for each direction, so the lesser value is always used in the figure. The thin lines are linear curve fits of the actuator's response at each preload, while the thick line represents the linear curve fit of all the data. The efficiency reported here is the cubic curve fit of the efficiencies calculated from all the data. The applied voltage in all cases was 3.5  $V_{RMS}$ .

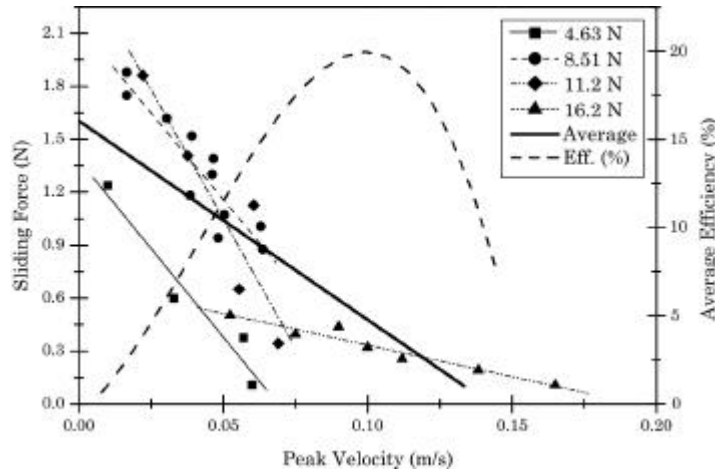


Figure 7: Sliding force and average efficiency versus sliding velocity with brake liner/alumina contact counterfaces. "Average" is a linear curve fit of all the plotted data points

From 4.63 N to 11.2 N of preload, the trend of the actuator's response is generally toward larger sliding force/peak velocities, but the higher 16.2 N preload gives a different response, with a dramatically higher peak velocity and reduced sliding force. This could possibly be to a change in the mode shape of the stator from redistribution of the contact force along the interface.

For an alumina/alumina contact interface, Figure 8 indicates the velocity versus time for a preload of 30.5 N and input voltage of 4.2  $V_{RMS}$ . Since the counterfaces are far stiffer, a higher preload is possible, which happens to require a higher applied voltage.

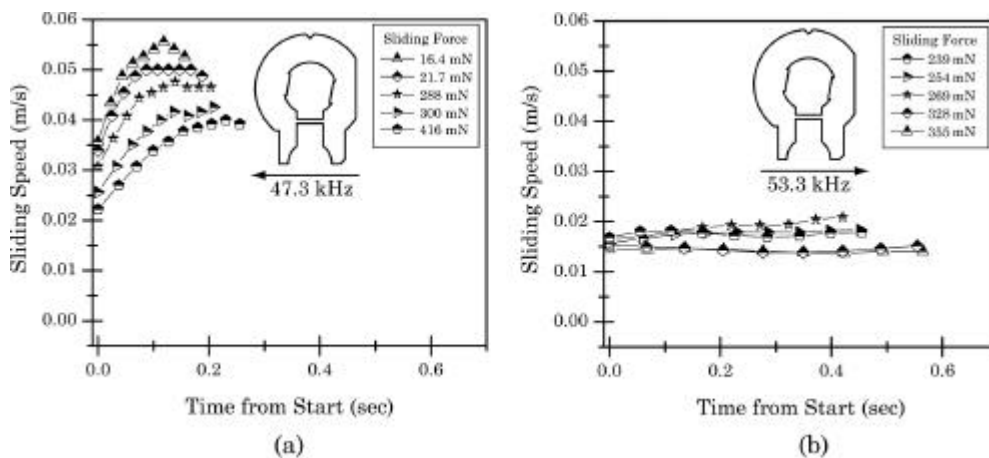


Figure 8: Velocity of slider versus time from start of sliding measurement for different sliding forces with alumina/alumina contact counterfaces, at (a) 47.3 kHz and (b) 53.3 kHz

Unlike the previous results, the response of the actuator using this contact interface is asymmetric with respect to direction. In the 47.3 *kHz* direction, this actuator appears to respond similarly to the brake liner/alumina actuator, but the 53.3 *kHz* direction has almost a constant velocity over the entire sliding range, regardless of the sliding force imposed on the system. Unfortunately, the efficiency of this particular configuration is consistently low at an average of 3.52%, with a standard deviation of only 2.2% over the entire range of sliding loads. However, the maximum force this actuator could deliver was 5.98 *N*, in either direction.

## CONCLUSIONS

A novel piezoelectric linear actuator was presented, using a single piezoelectric element mounted in the stator structure with swaging. The basic concept, along with its improvement via finite element analysis were shown. For a few select choices of two different stator designs and three different contact materials, the impedance characteristics of the stator along with the performance of the actuator were measured. The experimental results demonstrate the feasibility of the design concept.

Bidirectional motion, with a maximum sliding force of 1.5 *N* and 13 *cm/s* were obtained with alumina/brake liner contact, with a maximum efficiency of 20%. Using an alumina/alumina interface, a maximum sliding force of 5.98 *N* and 5.5 *cm/s* were obtained, but at only 3.5% efficiency.

For future work, the authors would like to pursue the revision of this actuator to improve upon the design of the stator, using *hard* PZT multilayer piezoelectric actuators, and to investigate further the complex interaction between the stator, slider, and friction liner exhibited in this study.

## ACKNOWLEDGEMENTS

The authors would like to acknowledge the assistance of Dr. Takaaki Ishii, without whom this work would have been impossible. The authors also appreciate support of this work by grants 0-5-2G010867, 0-5-2G113786 from Honeywell, NSF grant CMS-9409937, and a Monbusho grant-in-aid.

## REFERENCES

- [1] S. Ueha and Y. Tomikawa, *Ultrasonic Motors – Theory and Applications*, vol. 29 of *Monographs in Electrical and Electronic Engineering*, Clarendon Press, Oxford, 1993.
- [2] Kenji Uchino and Kazumasa Ohnishi, "Linear motor," U.S. Patent Number 4,857,791, August 15, 1989, 7 Claims, Assignee: Nissan Motor Co., Ltd., Yokohama, Japan Alps Electric Co., Ltd., Tokyo, Japan.
- [3] Kazumasa Ohnishi, Koichi Naito, and Toru Nakazawa, "Ultrasonic wave linear motor," U.S. Patent Number 5,216,313, June 1, 1993, 1 Claim, Assignee: Alps Electric Co., Ltd., Tokyo, Japan.
- [4] Timothy Swindle, Ara Chutjian, John Hoffman, Jim Jordan, Jeffrey Kargel, Richard McEntire, and Larry Nyquist, "Isotopic analysis and evolved gases," in *Planetary Surface Instruments Workshop*, T. Kostiuk C. Meyer, A. Treiman, Ed., Houston, Texas, USA, 1996, vol. 95-05, pp. 21-40.